Solar Energy 157 (2017) 263–276

Contents lists available at ScienceDirect

Solar Energy

journal homepage: www.elsevier.com/locate/solener

Mission profile characterization of PV systems for the specification of power converter design requirements

João M. Lenz [a,*], Hamiltom C. Sartori [b], José R. Pinheiro [a]

[a] Power Electronics and Control Research Group (GEPOC), Federal University of Santa Maria – UFSM, Av. Roraima, 1000, Prédio 7, Anexo B, CEP 97105-900 Santa Maria, RS, Brazil
[b] Integrated Regional University – URI, Av. Assis Brasil, 709, CEP 98400-000 Frederico Westphalen, RS, Brazil

ARTICLE INFO

Article history:
Received 22 February 2017
Received in revised form 7 July 2017
Accepted 7 August 2017
Available online 20 August 2017

Keywords:
Mission profile
PV converter design
Energy yield
PV operation analysis

ABSTRACT

This paper presents a comprehensive methodology to characterize the mission profile of photovoltaic systems, through which a powerful set of relevant information may be obtained and used in order to improve the design of power converters. Characterizing a photovoltaic system accurately is not trivial and this paper aims to present a detailed methodology on how to obtain a PV real field mission profile. Three cities with different climate were considered and a large dataset of four variables was used: global horizontal, direct, and diffuse irradiances and ambient temperature. Data were measured at one-minute intervals over multiple years. For each location, four scenarios of panel orientation were analyzed: horizontal position, fixed tilt, 1-axis and 2-axis mechanical tracker. A mathematical model to estimate instantaneous in-plane irradiance based on measured data and mounting type was used. An average profile of solar energy and ambient temperature for each city were built; these profiles were used as input for estimation of annual energy yield of a commercial photovoltaic panel, which was mathematically modeled and validated. Current and power processing throughout a year in a one-minute resolution were investigated, along with the most frequent and most significant operating points in each scenario. Panel operating temperature related to ambient conditions and its relation to energy yield were also studied. Finally, a comprehensive discussion to understand how different mission profiles affect power processing of photovoltaic power converters and the way this characterization can aid in pre-sizing and lifetime analysis of power electronics is presented.

1. Introduction

Long-term effective and reliable systems are one of the next big challenges in photovoltaic (PV) energy. Cost competitiveness is still one of the impeditive factors in PV industry when compared to conventional power plants. Modules and balance of system (BOS) correspond to 50% of a solar power plant cost (SPE, 2016), being the inverter responsible for a considerable amount of this total. The cost of energy (COE) of PV systems is highly dependent on the DC/DC converter and inverter (IRENA, 2012), not only due to installation costs but also for processing energy throughout the year in various ambient conditions. Case studies frequently show that these converters are still the element most prone to failure in PV systems and therefore, the design of more reliable power converters is a necessity (Ristow et al., 2008; Zhang et al., 2012).

Power converter's efficiency and reliability are key elements for expanding PV installed capacity and should be taken into account in solar energy estimation and in its design phases. Thus, in order to maximize energy yield, one must design and size a power converter according to the PV system characteristics and its generation profile. Instantaneous power delivered by PV power plants is dependent on several factors, such as solar irradiance, ambient temperature, module orientation and mounting type, solar cell performance, etc. (Rhodes et al., 2014; Vergura, 2015). Previous knowledge of *in situ* characteristics becomes essential for a correct system design, since inaccuracies in calculating rated and maximum values of energy yield may propagate through all design stages.

Modern design methodologies for PV DC/DC converters and inverters are focused on multi-criteria improvements, such as an increase in energetic efficiency, reduction of volume and/or cost, and an increase in lifetime. Optimization techniques for choosing the appropriate components technology and operating point have been proposed in order to enhance power density (Sartori et al., 2013; Scarpa et al., 2011). The trade-off between efficiency and

* Corresponding author.
E-mail addresses: joaomlenz@gmail.com (J.M. Lenz), hamiltomsar@gmail.com (H.C. Sartori), jrenes@gepoc.ufsm.br (J.R. Pinheiro).

http://dx.doi.org/10.1016/j.solener.2017.08.020
0038-092X/

Nomenclature

I_{cell}	PV cell output current
I_{λ}	photocurrent
I_{RSH}	shunt current
I_D	diode current
I_S	reverse diode current
V_{cell}	PV cell output voltage
R_{SH}	shunt resistance
R_S	series resistance
k	Boltzmann constant
q	electron charge
a_D	diode's ideality factor
FF	fill factor
T_{cell}	PV operating temperature
T_{amb}	ambient temperature
$\hat{\mathbf{i}}, \hat{\mathbf{j}}, \hat{\mathbf{k}}$	orthogonal unity vectors along the Zenith, East, and North axes
T_{NOCT}	PV temperature at NOCT
G^{PV}	irradiance on PV module
G_{NOCT}	irradiance at NOCT
PTR	Petrolina
IZA	Izaña
LIN	Lindenberg
TAY	Typical Average Year
α	sun elevation
φ	sun azimuth
$\vec{\mathbf{S}}$	sun position vector
β	PV panel tilt angle
γ	PV panel azimuth
$\mathbf{N}$	PV panel normal vector
z, e, n	Zenith, East, and North
θ_i	incidence angle between the Sun position and PV module normal vectors

power density was also studied by Kolar et al. (2009) in an optimized design for a PFC dual-boost converter, where maximum efficiency was analyzed at the rated power.

Even though photovoltaic generation is somewhat unpredictable on very short term, it hardly operates at the system's rated power. As thoroughly discussed by Dupont et al. (2012); Klein et al. (2009), contribution in PV energy is higher at mid-range solar irradiance levels. For this reason, Beltrame et al. (2014) proposed an optimum design of a PV boost converter where the operating point, magnetic materials, and semiconductors were selected in a database to increase annual power processing. By matching the DC/DC converter's efficiency curve with local weighted average solar irradiation, the boost's performance is greater in the most frequent irradiance levels.

Lifetime improvement of power electronics is becoming a demand in PV industry and different approaches have been proposed in recent years to design more robust and reliable converters and inverters applied in photovoltaics. A reliability-oriented design guide was proposed in (Wang et al., 2013) aiming to increase long-term operation of a transformerless PV inverter, where an analysis was performed to select the input capacitor bank with minimum overall stress and maximum lifetime. According to a five-year study in a large PV power plant (Moore and Post, 2008), PV inverters were the element responsible for most of the unscheduled maintenance and repair cost.

In this context, designing and manufacturing more reliable and more efficient power converters is crucial for enhancing a photovoltaic power plant cost-effectiveness. An accurate characterization of the PV mission profile should be the first step for any analysis involving reliability and pre-design, since knowing the available energy profile allows to understand the electrical and thermal behavior in which a power converter and its elements will operate.

A mission profile (MP) is a simplified representation of relevant conditions that the system in focus will be exposed in its intended application (ZVEI, 2008). In photovoltaic systems, MP can be defined as a dataset of annual power generation, energy estimation, environmental, and graphical results; from these, designers are able to extract the minimum, average, and maximum current, voltage, and temperature values in which the PV system will operate and build a relevant operation map. A detailed MP serves to accomplish different analysis, such as defining the optimum orientation for a PV power plant, performing financial feasibility studies, choosing and sizing an adequate PV modules and power converters and inverters, among other aspects. Previously characterizing the PV mission profile enables a comprehensive pre-design phase and supplies the designer with a valuable set of knowledge that can lead to enhancing the overall performance of photovoltaic energy processing. In addition, a power generation system can only be optimized in relation to the knowledge of its specific MP.

The effect of different MPs due to climate variation in different locations on the reliability of a PV push-pull was analyzed by De Leon-Aldaco et al. (2015), using local measurements of irradiation, temperature, and humidity. Diodes and capacitors presented higher failure rates and more susceptibility to thermal stresses. Definition of a real PV mission profile was also studied by Sintamarean et al. (2014), where an oriented PV inverter design based on silicon carbide was used. Solar irradiance and ambient temperature served as a base for estimation of a one-year PV system operating curves, which were then combined with thermo-electrical models for reliability evaluation. However, only data of horizontal solar irradiance was used and solely from one-year measurements.

Array and PV inverter sizing methodologies also benefit from the PV MP definition, as the one proposed by Mondol et al. (2006); the authors presented a correlation between optimum sizing ratio and PV/inverter cost ratio as functions of insolation and inverter type. Multiple factors for different European locations were considered, such as orientation and inclination, tracking mechanism, insolation, total system output, among others. Typically, the sizing ratio to maximize energy produced per system investment ranges from close to 1 to approximately 2 (Peippo and Lund, 1994) and different approaches have been proposed to find the ideal PV/inverter ratio. An analytical method for calculating the optimum inverter size in grid-connected PV plants was proposed by Demoulias (2010) using two observations: that the DC power of a PV plant can be represented as a straight line and that the efficiency curve of any inverter can be accurately defined by deriving three parameters from datasheet information. In contrast, a method to find the optimum PV plant for a specific inverter was presented by Faranda et al. (2015) through the extraction of a general efficiency curve for different DC/AC converters. All these methodologies rely on both solar irradiation data and PV power estimation, and they provide a useful tool for sizing PV arrays and inverters under different points of view. However, an optimum choice can only be made for a specific scenario and if the designer

has a full understanding of the system in focus. The methodology proposed in the present paper brings a fresh scope on PV energy analysis since mission profile characterization adds new information and tools for performing multiple design steps: array and inverter sizing, reliability and lifetime analyses, topology and technology selection, efficiency and energetic optimization, among others.

Thus, characterization of local mission profile is essential for designing high-performance power electronics in photovoltaic systems and a customized design maximizes energy yield. Available solar energy, in-plane irradiance, and ambient temperatures are some of the key variables needed for this kind of task. This paper proposes a detailed methodology for characterizing real field PV operating curves, based on long period of data measurements, as shown in Fig. 1. A PV modeling to estimate operating voltage and current concerning varying conditions of temperature and incident irradiance was performed. A mathematical model to determine the in-plane irradiance for panels in fixed mounting and with mechanical tracking was used. An analysis was carried out to determine which the optimum tilt angles for fixed tilt and 1-axis tracker mountings are, in order to estimate a real field MP with maximum PV energy generation.

Three locations with different climate were considered and the impact of different mission profiles on energy production was analyzed. For each studied scenario, output PV voltage, current, and power in a one-minute resolution were estimated throughout a year. A discussion about the importance of obtaining such a customized mission profile, and to comprehend how different MPs affect energy yield and power converter performance is presented.

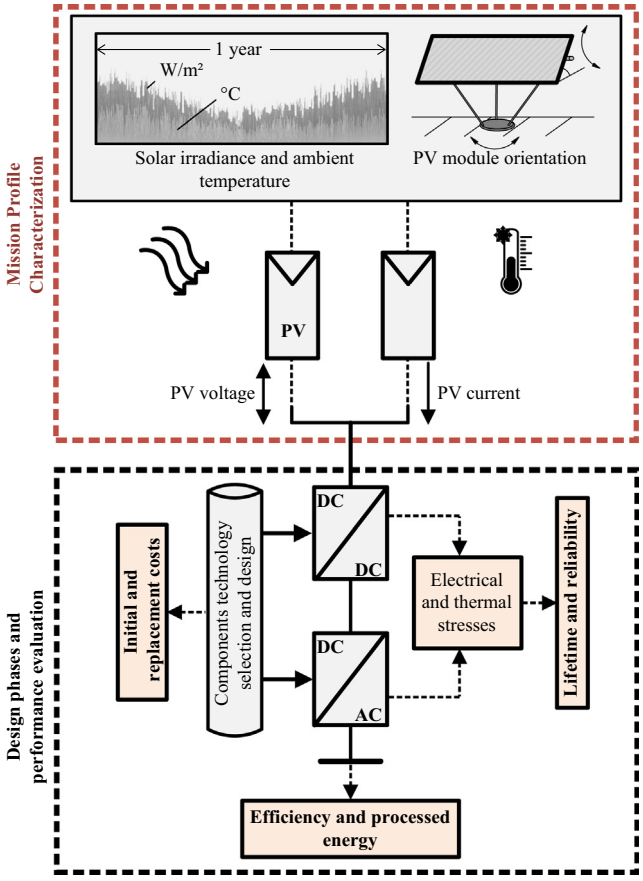

Fig. 1. Proposed characterization of the PV mission profile through multiple variables.

2. Photovoltaic modeling

In order to estimate correctly the energy processed annually by an inverter at a specific location, the solar cell was mathematically modeled to determine output power, current, and voltage of a PV panel for different conditions of irradiation and temperature. The well-accepted one-diode equivalent circuit for a PV cell shown in Fig. 2 was used, where a current source emulates the current generated by the photoelectric phenomenon, and the diode represents the semiconductor's non-linear characteristics. Losses are represented both by shunt and series resistances, R_{SH} and R_S, where the former represents the effects of internal leakage current and the latter is ohmic losses from PV's metallic conductors.

Analysis of Fig. 2 gives that the PV cell output current (I_{cell}) is obtained by

$$I_{cell} = I_{\lambda} - I_D - I_{RSH} \tag{1}$$

where I_{λ} is the photocurrent, I_{RSH} is the current due to losses in parallel resistance, and I_D is the current flow in the cell's intrinsic *p-n* junction.

2.1. PV cell model

A commercial module from Sun Earth® was used for modeling and validating the studied PV system, the model TPB 235 W with polycrystalline cells was chosen due to availability for experimental testing and for having an adequate amount of datasheet information – the following methodology can be reproduced for any panel manufacturer or module type. Main characteristics of the used panel are shown in Table 1, for standard test conditions (STC).

Modeling of the equivalent circuit, displayed in Fig. 2, consisted of finding four key parameters: diode's reverse saturation current (I_S), shunt and series resistances, and diode's ideality factor (a_D). Since the panel output current is non-linearly dependent on the output voltage, V_{PV}, (1) can be rewritten as (2) and an iterative method is needed to solve this transcendental equation.

$$I_{cell} = I_{\lambda} - I_S\left(\exp^{\left(\frac{q(V_{cell}+R_S I_{cell})}{kT_{cell}a_D}\right)} - 1\right) - \frac{V_{cell} + R_S I_{cell}}{R_{SH}} \tag{2}$$

where V_{cell} and I_{cell} are the voltage and current, respectively, of a single photovoltaic cell, q and k are the electron charge ($q = 1.602 \times 10^{19} C$) and the Boltzmann ($k = 1.38065 \times 10^{23} J/K$) constants, and T_{cell} is the PV cell temperature, in Kelvin.

The methodology proposed by Villalva et al. (2009) was used for determining I_S, R_{SH}, and R_S, through the values exposed in Table 1. An initial guess of the shunt resistance was set and the iterative process of I_S, R_{SH}, and R_S was conducted until the maximum power point (MPP) at STC was calculated with an error less than 0.5%. According to (Villalva et al., 2009), the dimensionless ideality factor can be parametrically adjusted, thus, in this paper, a first estimation of a_D was set as the $I \times V$ curve fill factor (FF) inverse, as in (3). The calculated parameters for the described model are presented in Table 2.

$$a_D = FF^{-1} = \frac{V_{OC}^{STC} I_{SC}^{STC}}{V_{MPP}^{STC} I_{MPP}^{STC}} \tag{3}$$

where V_{OC}^{STC} is the open circuit voltage, I_{SC}^{STC} is the short-circuit current, and V_{MPP}^{STC} and I_{MPP}^{STC} are the MPP voltage and current, respectively. Assuming that $I_{\lambda} \approx I_{SC}$ and with the initial guess for a_D given by (3), I_S, R_{SH}, and R_S were calculated by solving (2) through and an iterative process (Villalva et al., 2009). Afterward, a parametrical adjustment on the ideality factor was done with the objective to minimize the V_{MPP}^{STC} error relative to the datasheet value.

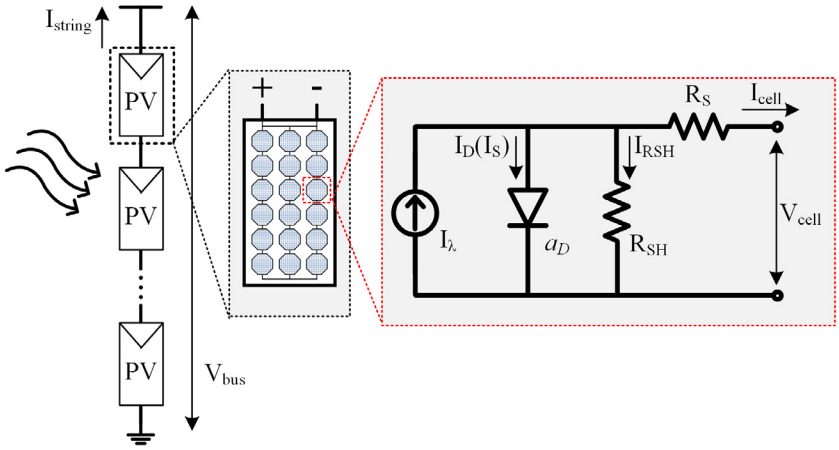

Fig. 2. Solar cell parameters and the one-diode equivalent circuit.

Table 1
Sun Earth® TPB 165 × 165–60-P 235 W datasheet information.

Parameter	Value	Description
I_{SC}^{STC}	8.47 A	Short-circuit current
I_{PV}^{MPP}	8.05 A	Current @ maximum power point
V_{OC}^{STC}	36.7 V	Open circuit voltage
V_{PV}^{MPP}	29.2 V	Voltage @ maximum power point
P_{MPP}^{STC}	235 W	Maximum power
μ_P	−0.45%/°C	Power temperature coefficient
μ_V	−0.35%/°C	Open voltage temperature coefficient
μ_I	0.05%/°C	Short-circuit temperature coefficient

Table 2
Sun Earth® TPB 165 × 165–60-P 235 W modeled parameters.

Parameter	Value	Description
R_{SH}	648.76 Ω	Shunt resistance
R_S	0.145 Ω	Series resistance
I_{S0}	1.2783×10^{-7} A	Diode reverse saturation current
a_D	1.312	Diode ideality factor

2.2. Panel operating temperature

Photovoltaic efficiency decreases with the rise of operating temperature, as discussed in the literature (Accetta et al., 2012; Coelho et al., 2009; Rahman et al., 2014; Skoplaki and Palyvos, 2009b); in this paper the well-accepted model described by (4) was chosen for estimating cell operating temperature (T_{cell}). Although simple, this model is considered accurate for calculating T_{cell} in function of incident irradiance and ambient temperature, for crystalline silicon PV cells (Skoplaki and Palyvos, 2009a).

$$T_{cell} = T_{amb} + (T_{NOCT} - T_{a,NOCT})\frac{G^{PV}}{G_{NOCT}} \quad (4)$$

where T_{amb}, T_{NOCT}, and $T_{a,NOCT}$ are the ambient temperature, normal operating cell temperature (NOCT), and ambient temperature at NOCT, respectively; G^{PV} and G_{NOCT} are the irradiance on the module surface and the NOCT irradiance. The main issue of (4) is that it considers only steady-state temperature. In order to account for thermal dynamics and avoid abrupt temperature variations due to irradiance change, actual T_{cell} as an average between instantaneous and previous temperature values was estimated.

2.3. PV system validation

Each Sun Earth® model is composed of 60 (sixty) cells in a series connection, thus the PV panel output current was mathematically reproduced through (2) and the parameters of Table II. The $I \times V$ characteristic curve in function of the cell operating temperature and incident solar radiation was modeled for varying environmental conditions. In order to validate the PV modeling and energy estimates, simulated results were compared with long-term experimental measurements from a real photovoltaic plant. This system is composed of twenty-eight Sun Earth® Polycrystalline TPB 235 W modules equally divided in two parallel strings; each string has fourteen modules in series connection with a total of 3.29 kW installed power. The power plant is on a rooftop using fixed mounting, with a tilt angle of 24° towards North, located at S 29 °42′48.379″ and W 53 °43′2.5986″.

A central inverter (SMC 6000TL from SMA) performed MPPT, DC bus regulation, and energy processing. An instrumentation system measured current and DC bus voltage; ambient and PV module temperatures, and in-plane irradiance; one-second measures were acquired and one-minute averages were stored. String current and DC bus data were compared with simulation results in order to validate the PV modeling. Estimated and measured current and voltage are depicted in Fig. 3 where three days with different irradiance and temperature conditions are highlighted.

Discrepancies found from measured results can be explained, mainly, by the fact that the MPPT carried out by the inverter is non-ideal and the real system may not be operating exactly at the MPP. The MPPT also tends to operate less effectively at low irradiances, which may explain why the model is significantly overestimating in very-low-power conditions. In addition, possible mismatch and soiling of PV panels in each string were not included, which can cause difficulties for the central inverter to find the global maximum power point.

A scatter plot of the estimated power versus measured values is shown in Fig. 4, where each point represents PV string power in one-minute. Although simulation results seemed to overestimate the power produced by the PV string, there is an evident relationship between estimated and experimental values.

Furthermore, the PV operating temperature is another source of possible inconsistencies in the obtained results since both the PV module efficiency and output voltage are highly dependent on the solar cell temperature. Despite being widely used, the present paper is limited to the model of (4) to estimate the PV module temperature; this model does not take into consideration cooling caused by the wind, heat transfer or any other thermal dynamics. A more sensible and complex approach for estimating the PV operating temperature should improve the presented results, but it is out of this paper's scope.

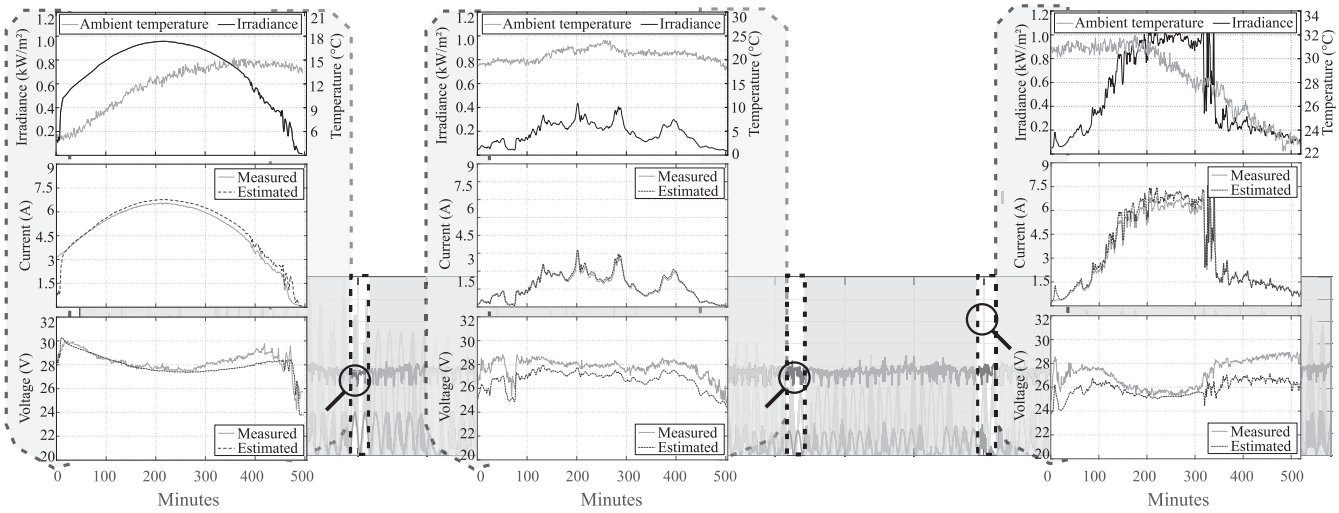

Fig. 3. $I \times V$ curve of modeled PV panel validated according to datasheet information and compared with experimental measurements for varying seasonal conditions of irradiance and temperature.

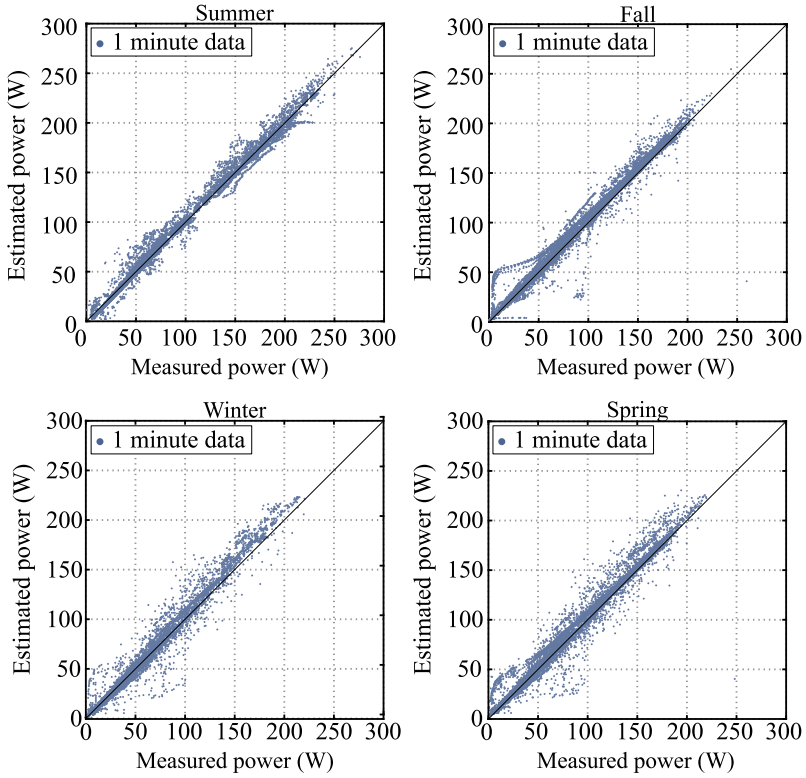

Fig. 4. Comparison between simulated and experimental PV maximum power for various conditions of irradiance and temperature.

Although neglecting these aspects, the PV string generated energy measured was of 1.615 MWh, while estimated was equal to 1.654 MWh, resulting in an overall error of 2.43%. Mean Absolute Error (MAE) for power, voltage, and current estimates were calculated by (5) and normalized with respect to the mean measures of each variable.

$$MAE = \frac{\sum_{i=1}^{n} |y_i - x_i|}{n} \tag{5}$$

where n is the number of data analyzed, and y and x are the estimates and measurements. Normalized MAE of power, voltage, and current were equal to 0.0654, 0.0496, and 0.0465, respectively.

3. Local variability and meteorological data

Solar energy maps and databases are useful for feasibility analysis and assessing PV energy in locations with none or small data availability, as in Huld et al. (2012), Khan and Ahmad (2012); while forecasting techniques are valuable tools for operating plants and making short-term decisions, as presented by Chen et al. (2011) and Gulin et al. (2017). However, in order to maximize energy harvesting, good quality data and from long periods must be used in the design stages of photovoltaic systems and its power converters. Uncertainties in solar data can make the difference between profit and loss (Paulescu et al., 2013), especially in large-scale PV plants with high financial investments.

In this paper, data from three meteorological stations were used; these stations are under the responsibility of various climate/weather agencies and belong to the Baseline of Solar Radiation Network (BSRN). Further information on data quality and retrieval are available via (WRMC-BSRN, 2017).

3.1. Dataset and quality check

In order to investigate the impact of weather variability on photovoltaic energy, three locations with distinct climates were analyzed. Furthermore, these cities were chosen for having certified BSRN stations with a long period of available data and being fully equipped for radiometric measurements. These stations are localized at Petrolina (PTR), Brazil, Izaña mountain (IZA), Tenerife, Spain, and Lindenberg (LIN), Germany. Further information is described in Table 3.

Horizontal positioning is hardly employed in photovoltaic systems and clear sky is scarcely possible in normal weather conditions. Even though being unrealistic scenarios, global horizontal data and clear sky models are frequently used to design and analyze PV systems, as in Daut et al. (2011), Dupont et al. (2012), Sintamarean et al. (2014). To avoid inaccuracies, measured data of global horizontal, direct, and diffuse irradiances and ambient temperature was used.

Each of these four variables was recorded in a one-minute resolution along with a timestamp, totaling more than two million data points per year per location. A ten-year period dataset was collected from PTR and an eight-year period from LIN and IZA, which ensures a precise set of data.

Since stations that belong to the BSRN are required to undergo calibration and standard checks, data of each considered variable was submitted to a quality control process. A two-step procedure to examine data quality was realized through BSRN Toolbox (Schmithüsen et al., 2012) and the following quality checks were done:

i. Verify and flag if a sample is outside physically possible limits;
ii. Verify and flag if a sample is physically possible but extremely rare;

The limits and quality control recommendations presented by Long and Dutton (2004) were used.

3.2. Typical average year

According to the previously described instructions, data samples that failed the physically possible and extremely rare tests were discarded. In order to maintain the consistency of measurements, all samples in the same minute were excluded if one variable failed the quality test; *e.g.*, if a diffuse irradiance measurement was outside the physically possible limit, all other data in that same minute were discarded and considered as not a number.

For each analyzed city, a long-term dataset of four variables in one-minute measurements was formed. With such a large span of time and data, it was possible to obtain a representative annual profile of both solar irradiance and ambient temperature. Due to climate long-term variability and weather short-term randomness, the large dataset used in this paper favors the analysis under the perspective of the average operating conditions at each location, in a period length relevant to the PV plant lifetime.

The Typical Average Year (TAY) was obtained by grouping and averaging the variables of interest according to the timestamp in which they were measured. Minute-by-minute measurements of irradiance (horizontal, direct, and diffuse) and ambient temperature were placed in separate arrays; in order to obtain equally sized arrays (525,600 min for each year), additional days of leap years were discarded. After this data handling, the Typical Average Year was formed by taking the minute average of all samples within the same array position (same timestamp) across each year with available data. Thus, TAY of each location is a 4×525600 matrix, and its values are the representative average condition of each variable throughout the year.

3.3. Irradiation and temperature profile

In order to observe and illustrate the difference between profiles of all irradiances and temperature from each location, Fig. 5 depicts the daily averages of all variables obtained from the calculated TAY. Available solar energy in the TAY in relation to irradiance level is depicted in Fig. 6, alongside annual irradiance on the ground surface. The differences between the analyzed profiles permit to characterize how different ambient conditions affect PV generation and distinct elements of power processing units.

4. PV mounting and positioning

Accurate estimation of photovoltaic energy production is not a trivial task since it relies on the precision of multiple models and datasets combined. In this paper, available datasets of solar energy and a Sun path calculation algorithm were used as input; afterward, a mathematical model is used to determine PV panel orientation relative to the ground and the incidence angle between Sun and PV surface. Finally, a photovoltaic cell model to estimate output power throughout one-year operation was used.

4.1. Surface irradiance incidence

Evaluation of annual irradiance incidence on a PV module with fixed mounting, or mechanical tracking was done through a multiple-step algorithm summarized as follows:

1. **Calculate the Sun angular path** for each location and for a whole year, in high-resolution, with reference to a coordinate system centered on the PV panel, with North-South, East-West, and Zenith axes;
2. **Determine the module angular position vector**, $\vec{N}$, in the same coordinate system, where:
   2.1 Mechanical tracking is simulated by making the PV panel azimuth (γ) continuously follow the Sun's azimuth (φ);
   2.2 Module's azimuth is oriented due South for northern hemisphere locations (IZA and LIN), and due North for PTR;

Table 3
Station information.

Station	Latitude	Longitude	Elevation	Number of months with data
PTR	09°07′S	40°32′W	387 m	119
IZA	28°31′N	16°50′W	2373 m	87
LIN	52°21′N	14°12′E	125 m	80

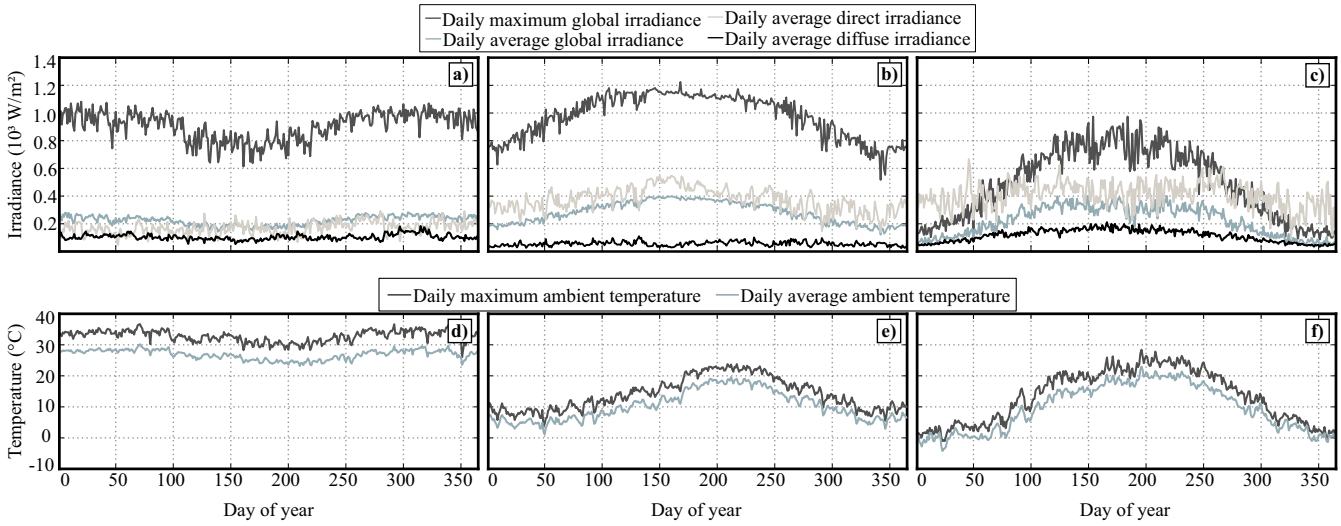

Fig. 5. TAY profile for solar irradiance from (a) Petrolina, (b) Izaña, and (c) Lindenberg, and ambient temperature from (d) Petrolina, (e) Izaña, and (f) Lindenberg.

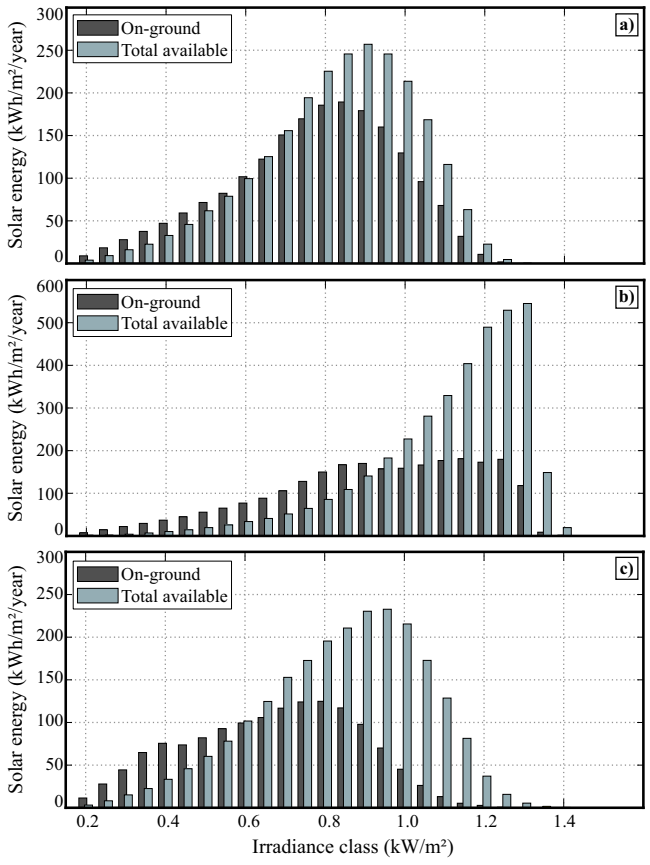

Fig. 6. Solar radiation at (a) Petrolina, (b) Izaña, and (c) Lindenberg in different irradiance levels in the TAY.

2.3 An optimum tilt angle is used for fixed and 1-axis tracking configuration, and for a 1-axis tracking system following the Sun azimuth;

3. **Calculate the incidence angle between Sun and module**, minute by minute per year for all mounting configurations, and estimate the total quantity of solar irradiance on the PV panel surface using the radiometric data.

Geometry needed for incidence angle determination is illustrated in Fig. 7, wherein key elements are the Sun vector position and the surface normal vector. Mounting configuration determines the value of the tilt angle between ground and PV panel, β, and if the module's azimuth is fixed or variable.

Calculation of Sun vector position, $\vec{\mathbf{S}}$, in relation to the observer is a well-discussed subject in literature and different methodologies can be used according to the precision needed. In this study, equations presented by Reda and Andreas (2008) were used as a reference for developing an algorithm to calculate Sun's elevation and azimuth angles (α and φ, respectively) in function of time. Incidence angle between the PV surface and Sun was calculated as (5), while instantaneous irradiance was estimated according to (7)–(9),

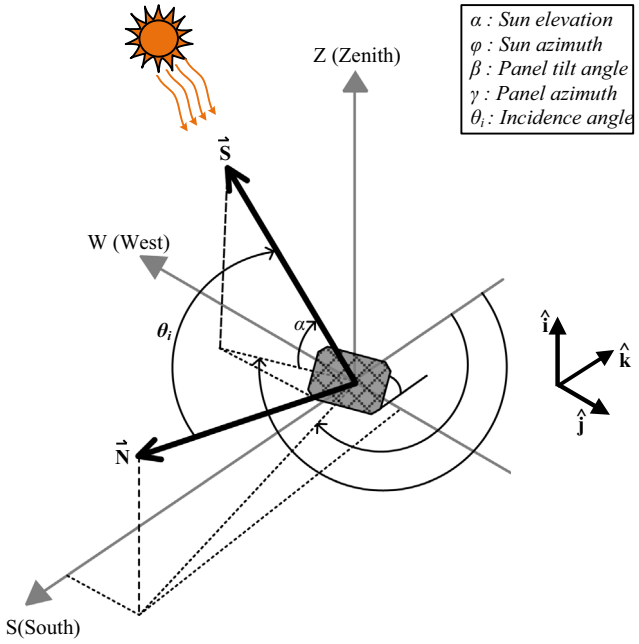

Fig. 7. Geometry for calculating solar irradiance incident angle on an arbitrarily oriented surface.

$$\theta_i = \cos^{-1}(\vec{\mathbf{S}} \cdot \vec{\mathbf{N}}) \tag{6}$$

$$G^{PV}_{direct} = G_{direct}\cos(\theta_i) \tag{7}$$

$$G^{PV}_{diffuse} = G_{diffuse}\left(\frac{1+\cos(\beta)}{2}\right) \tag{8}$$

$$G^{PV} = G^{PV}_{direct} + G^{PV}_{diffuse} \tag{9}$$

where θ_i is the incidence angle between Sun and PV module, G_{direct} and $G_{diffuse}$ are the measured data of each irradiance type and G^{PV}_{direct}, $G^{PV}_{diffuse}$, and G^{PV} are the estimated, direct, diffuse, and total irradiance incidence over the panel surface. Reflected irradiance was not considered due its contribution to total solar irradiance is many times smaller than the direct and diffuse components, besides being more complex to model since reflection is dependent on the surroundings specific geographical characteristics. Main steps used for PV energy estimation and mission profiling are depicted in Fig. 8.

Calculation of the position vectors, $\vec{\mathbf{S}}$ and $\vec{\mathbf{N}}$, is done through (10) and (11), where $\hat{\mathbf{i}}, \hat{\mathbf{j}}, \hat{\mathbf{k}}$ are unit vectors along the Zenith (z), East (e), and North (n) axes. The components of each position vector along the z, e, and n axes can be obtained through (10.1) and (11.1) by geometrically solving Fig. 7.

$$\vec{\mathbf{S}} = S_z\hat{\mathbf{i}} + S_e\hat{\mathbf{j}} + S_n\hat{\mathbf{k}} \tag{10}$$

$$\begin{cases} S_z = \sin(\alpha) \\ S_e = \cos(\alpha)\sin(\varphi) \\ S_n = \cos(\alpha)\cos(\varphi) \end{cases} \tag{10.1}$$

$$\vec{\mathbf{N}} = N_z\hat{\mathbf{i}} + N_e\hat{\mathbf{j}} + N_n\hat{\mathbf{k}} \tag{11}$$

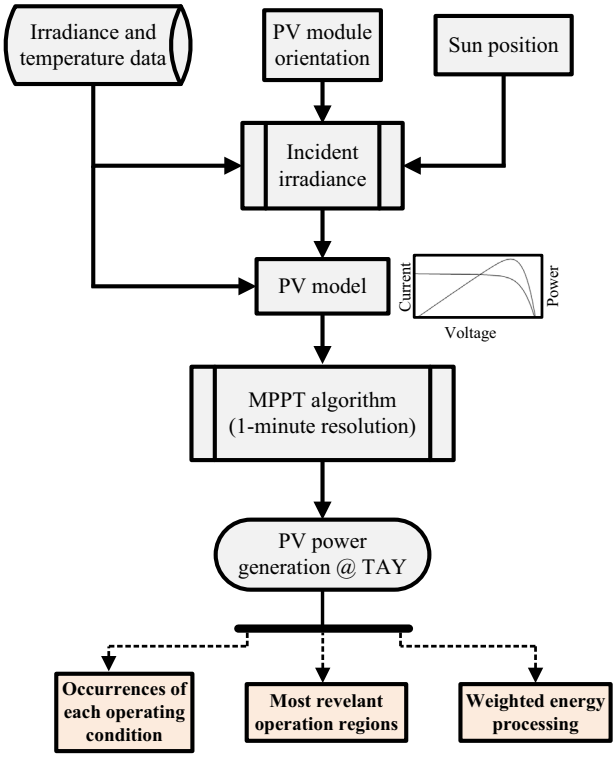

Fig. 8. Steps of the proposed methodology for photovoltaic energy estimation.

$$\begin{cases} N_z = \sin(\beta) \\ N_e = \cos(\beta)\sin(\gamma) \\ N_n = \cos(\beta)\cos(\gamma) \end{cases} \tag{11.1}$$

where S_z, S_e, S_n and N_z, N_e, N_n are the Zenith, East, and North components of the Sun position vector ($\vec{\mathbf{S}}$) and PV module normal ($\vec{\mathbf{N}}$), respectively.

4.2. Incidence angle of moving surfaces

A mechanical tracker model for PV systems requires the Sun's annual angular path for the location of interest and its respective position vector ($\vec{S}$) in function of time, as described in Section 4.1. The movement of PV modules can be estimated through varying the panel's tilt angle (β) and/or azimuth (γ) in time. This will result in two time-varying position vectors, $\vec{S}$ and $\vec{N}$, which can be solved through (10) and (11), respectively.

Different types of tracker mechanisms (Clavijo, 2012; Grupo. Clavijo, 2012; Meca Solar, 2014a; Meca Solar, 2014b) and control strategies (GmbH, 2015; Pesos.Solar.Products, 2015) are presented in the PV industry, varying from horizontal to polar mountings, from astronomical sun tracking to external radiation sensor-based. Since it is not the scope of this paper, factors such as mechanical tracking efficiency, drive losses, control accuracy and backtracking were not considered.

A single-axis tracker with tilted modules and a degree of freedom along the East/West axis is considered in the following sections, where tracking is accomplished by making the PV panel azimuth follow the Sun's. In dual-axis systems, both the panel's tilt and azimuth are movable and follow the Sun's respective angles, α e φ. A continuous tracking with null error is assumed in both scenarios.

4.3. Custom optimum tilt angle

Definition of the panel tilt angle with respect to ground may have a significant impact on annual energy processing. The most common practice adopted by PV contractors is outdated equations for calculating the tilt angle as a constant factor of the local latitude. Such methods, as Lewis (1987), Reindl et al. (1990), assume that climate and weather conditions are homogeneous for equal latitudes, which is far from true. An extensive study by Deb et al. (2007) demonstrated that PV panel positioning has a deep impact not only in annual irradiation but also in overall system efficiency and financial savings for a grid-connected system.

Tilt angle calculation performed by Chang and Yang (2012), Yadav and Malik (2015) was restricted by only 1-year of measured data, which might over or underestimate availability of solar energy if such period was influenced by abnormal climatic conditions. However, Chang and Yang (2012) used probability in order to reduce error and consider weather condition uncertainties. Urban topology was considered by Siraki and Pillay (2012) in an investigation to determine how the shadowing from nearby obstacles affected the optimum tilt angle in different latitudes, whereas (Freitas et al., 2015) used genetic algorithms to perform PV layout optimization to maximize energy yield.

By using a TAY considering several years of data, in this paper, it was possible to find a β_{opt} that satisfied the average profile of solar irradiation for each city, which avoids designing a PV system based on non-typical data. The surface positioning model depicted in Fig. 7 was used to find which tilt angle maximized the solar energy incidence for each mission profile.

For fixed mounting configuration, PV panel orientation was varied in order to determine the tilt angle and azimuth that resulted in

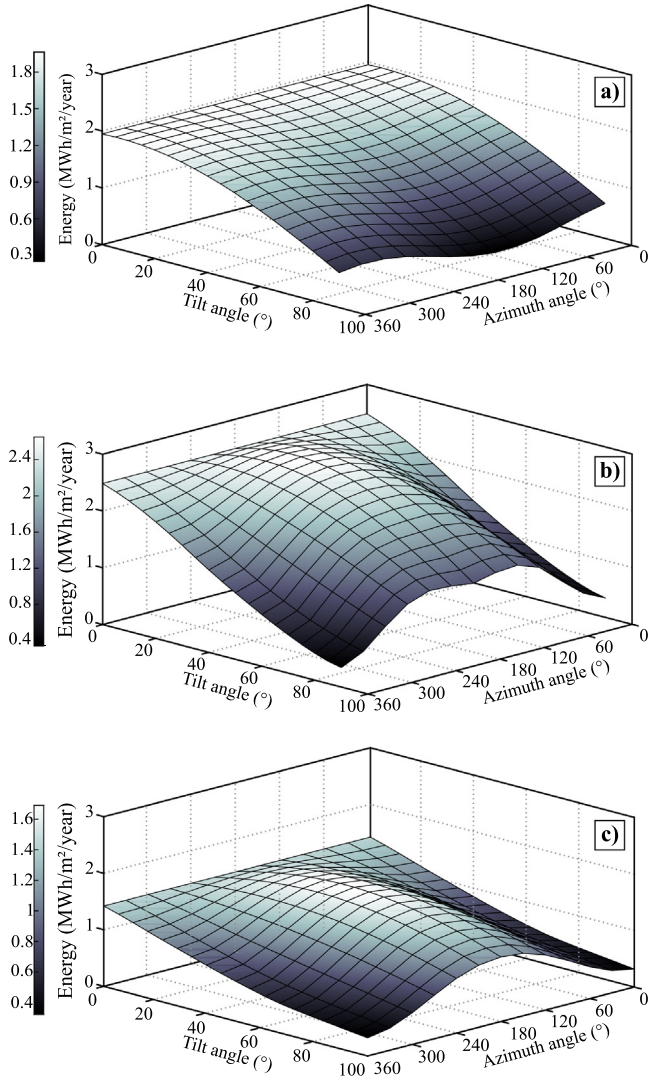

Fig. 9. In-plane solar energy incidence of fixed surface in function of tilt angle and azimuth orientation for (a) Petrolina, (b) Izaña, and (c) Lindenberg.

maximum solar irradiation. Annual irradiance incidence in function of β and φ is depicted in Fig. 9. Since obstacle shadowing was not included, true South resulted in the maximum solar incidence for IZA and LIN. At Petrolina, the azimuth orientation choice has a low impact for small tilt angles, since the city is located near the Equator line. Optimum orientation for each scenario is described in Table 4.

The tilt inclination for PV systems with 1-axis trackers is often disregarded and calculated with the same methods as in fixed

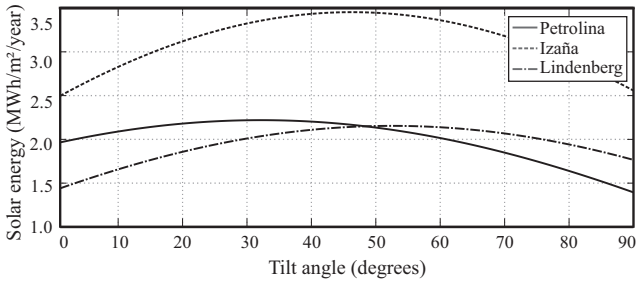

Fig. 10. Annual energy yield for varying tilt angle at Petrolina, Izaña, and Lindenberg, for 1-axis tracker.

mounting. Smaller tilt angle favors incidence during midday, where the Sun is at its highest position. Nevertheless, higher β favors morning and afternoon energy generation due to the Sun's smaller elevation. Thus, optimum tilt angle for single axis trackers is a trade-off and must be assessed for each specific application.

The relationship between tilt angle and annual solar incidence for single axis trackers is shown in Fig. 10. Optimum orientation angles for each mission profile are described in Table 4; energy generated by a single PV module in these conditions and energy gain compared to panels in a horizontal position is also presented Fig. 10.

5. Analysis of PV mission profile and energy generation

As previously demonstrated, the somewhat random and variable nature of irradiation and temperature has a deep impact on photovoltaic energy generation. The previous characterization of local conditions allows a comprehensive detailing of the energetic behavior to expect from a PV power plant. In addition, it also favors the improvement of energy processing since power converters can be optimally designed or specified to meet the application's particularities.

5.1. Operating points behavior

The input current is a key parameter for designing a power converter since rated and maximum values are essential for component specification, losses calculation, and other subsequent design stages. In addition, current levels are also crucial for reliability analysis due to its impact on the thermal and stress behavior of all main converter components.

Therefore, previous knowledge of PV panel current behavior, absolute maximums, and average curves are essential for characterizing photovoltaic mission profile. As summarized in Fig. 8, current and voltage profile is dependent on both irradiance incidence and panel temperature. Thus, PV operation in the TAY was estimated in a one-minute resolution, considering fixed mounting

Table 4
Optimum orientation and total processed energy in the Typical Average Year.

Location	Mounting type	Optimum tilt angle -	Azimuth angle	Single module generation in TAY (kWh)	Gain relative to horizontal surface
Petrolina, Brazil	Fixed	6°	0°	371.77	1.27%
	1-axis tracking	32°	–	419.24	14.20%
	2-axis tracking	–	–	432.64	17.85%
Izaña, Spain	Fixed	21°	180°	537.36	6.77%
	1-axis tracking	46°	–	707.63	40.60%
	2-axis tracking	–	–	745.83	48.19%
Lindenberg, Germany	Fixed	36°	180°	336.62	17.66%
	1-axis tracking	53°	–	417.51	45.94%
	2-axis tracking	–	–	430.90	50.62%

(horizontally and with fixed tilt) and use of mechanical trackers (1-axis and 2-axis), for each location described in Table III.

One-year operating current and voltage pair are shown in Fig. 11, where each pixel depicts a resolution of 100 mV by 100 mA, for the following scenarios:

i. ***PTR-2x:*** 2-axis tracker system in Petrolina, Fig. 11a and d;
ii. ***IZA-fixed:*** Fixed tilt with an optimum angle in Izaña, Fig. 11b and e;
iii. ***LIN-horiz:*** Horizontal position in Lindenberg, Fig. 11c and f.

Color scale in Fig. 11a–c represent the frequency of operation, in hours, for each $I \times V$ pair, while the heat map in Fig. 11d–f depict the amount of processed PV energy, in kWh. For a better visualization, only $I \times V$ pairs that occurred for at least 2 min and contributed with at least 50 Wh are depicted. These types of graphics may be called as Relevant Operation Maps of a studied PV system.

Due to its steadier and sunnier climate, Fig. 11a indicates that a PV system in Petrolina operates most frequently in a well-defined region of PV current ranging from 4 to 6 A; this region of $I \times V$ operation is the same region responsible for most of the power processing in a one-year period. For having a warmer climate and higher average ambient temperatures, lower MPP voltages are more significant, which indicates that an inverter with maximum efficiency in rated DC level is not favorable for *PTR-2x*.

In contrast, MPP voltages are most frequently found at higher values on the other locations, due to lower ambient temperatures, especially in Lindenberg. Results indicate that for *LIN-horiz*, occurrences of operating $I \times V$ are distributed in two different regions, wherein the most frequent condition of PV operation is not the same that produces the most output of PV energy.

Izaña station is situated at a high altitude and frequently above cloud level, resulting in lower levels of diffuse irradiance (Fig. 5b) and solar energy variability. This also explains the high energy gains due to the use of mechanical trackers (Table 4) since direct irradiance can be harvested more efficiently. In addition, the most frequent $I \times V$ region for *IZA-fixed* (Fig. 11b) is significantly thinner than the other considered profiles and produced PV energy is highly concentrated in short ranges on the $I \times V$ map.

The relationship between the most frequent and the most relevant operating condition for energy processing is vital for the optimum design of PV converters. Previous knowledge of a complete mission profile allows the designer to improve a converter's efficiency in the region where it will process more energy. Furthermore, long-term information of ambient conditions and

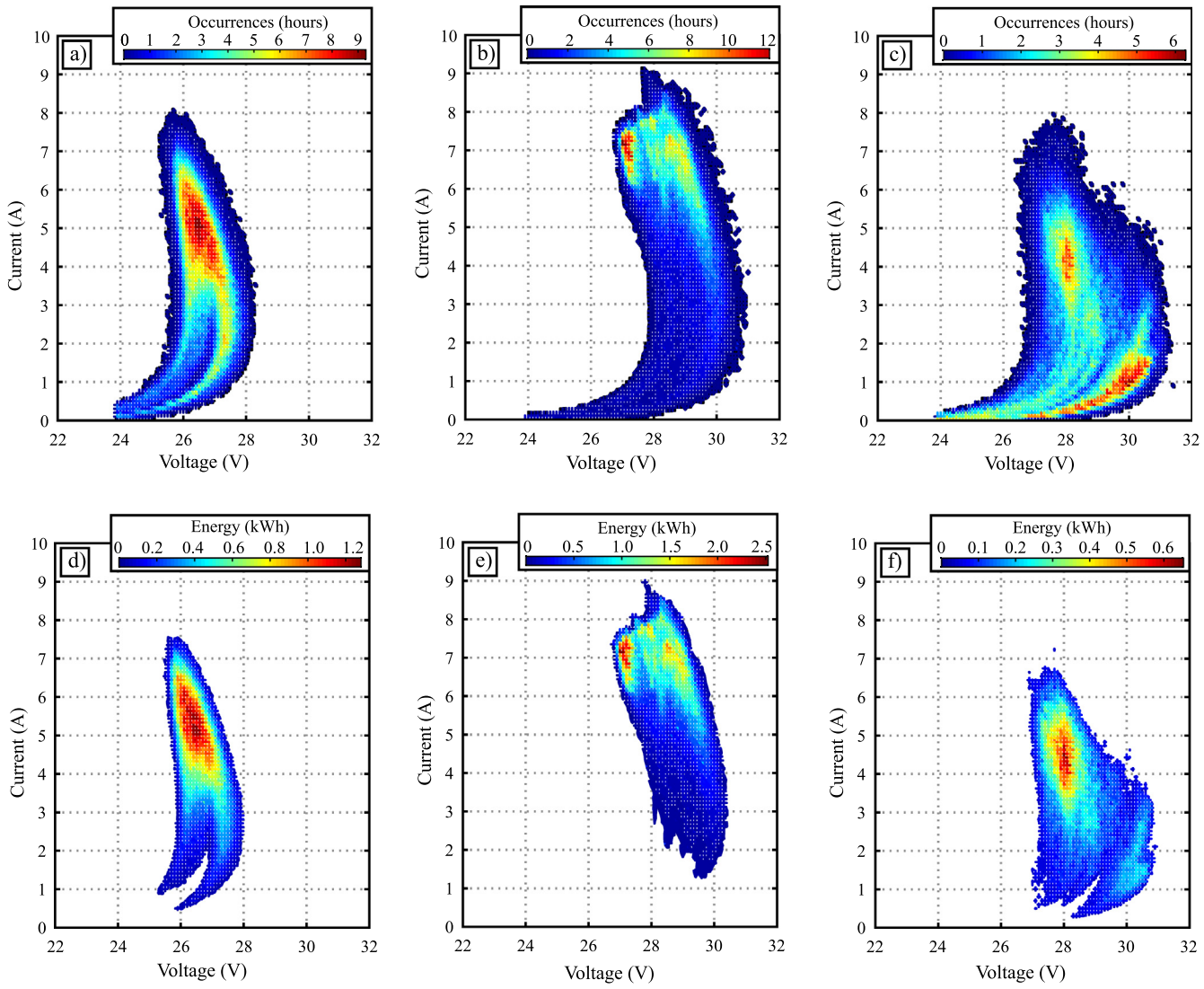

Fig. 11. One-year current *vs.* voltage operating points for a single PV module relative to occurrence frequency, in hours, for (a) Petrolina, (b) Izaña, and (c) Lindenberg; and relative to processed energy, (d), (e), and (f), respectively.

occurrences of different operating conditions allow a design for reliability (DfR) approach through a lifetime analysis of each power element in a PV system.

Analysis of Fig. 11 clearly demonstrates that different mission profiles, *i.e.* different levels of solar irradiation and ambient temperature have a significant impact on PV generation. Therefore, converter performance throughout the year is directly dependent on such variations, once that PV output values dictates the power processing characteristics.

Furthermore, panels mounting and positioning affect power processing, since PV mechanical tracking results in higher irradiance, current, and power levels. Lower variability in voltage is a consequence of *p-n* junction behavior of photovoltaic cells, while greater current variation is due to its current source characteristic.

5.2. Ambient temperature influence

Through the methodology proposed and discussed so far, an analysis was carried out to evaluate how the mission profile and ambient temperature affect PV panel output and its produced energy. Using the TAY from each location and the profiles described in the previous section, the relationship between ambient temperature and annual processed energy is depicted in Fig. 12.

Lindenberg is located in a temperate climate zone, with well-defined seasons and high thermal amplitude. For this reason, PV energy processing occurs along a wide range of ambient temperatures, with small distinction in Fig. 12. Meanwhile, at Petrolina, most of PV generation happens in a smaller range of higher temperatures, due to its tropical location closer to the Equator Line.

Despite the fact that it is located in a sub-tropical climate, Izaña's station high altitude favors great energy yield in low ambient temperatures, which is not a common feature in photovoltaic systems. This indicates that PV panels operate with higher conversion efficiency and power converters can process more energy with less thermal stress.

Ambient temperature is a crucial set of information and should be considered in the design phases of a PV power converter since its thermal behavior is dependent on the outside temperature. Steady-state and cyclical temperature is the main source of stress for power and electronic elements (ZVEI, 2008), increasing its failure rate. In order to enhance reliability, one must ensure that the selection and design of each component will sustain the mission profile's temperature dynamics.

5.3. Impact on energy processing

The mission profile oriented design of power electronics is capable of improving overall efficiency and reduce long-term costs, as this concept considers all main peculiarities that will rule energy processing. Recent works in this scope include considering semiconductor reliability in a PV inverter design (Sintamarean et al., 2014) and an optimization technique for a PV boost converter focusing on weighted average efficiency increase (Beltrame et al., 2014).

An accurate energy and mission profile is a key asset for developing high-performance photovoltaic power plants and converters. Conventional design of DC/DC converters aims to achieve higher efficiency at rated power. However, maximum powers are some of the least occurring events in PV applications due to weather variability. Techniques for design optimization aiming to improve annual energy processing, as in (Beltrame et al., 2013), rely on previous knowledge of accurate energy and mission profiles.

In order to understand which PV operating points contribute the most to energy generation, an analysis of the PV power plant previously described was conducted from the point of view of power processing during a one-year operation. Output current was grouped in ranges of 500 mA, assuming an ideal MPPT, and the annual processed energy was obtained through summing PV power in one-minute samples. Fig. 13 depicts energy yields in reason of operating MPP current for each location.

Because of its more variable climate, PV energy profile at Lindenberg with a fixed tilt mounting was distributed more evenly in the MPP current spectrum. This is consistent with the findings presented in Fig. 11f, where the $I \times V$ operation regions more relevant for power processing are not concentrated. The use of mechanical trackers increases PV energy generation and concentrates the relevant MPP current on a thinner region. It is also noticeable that even though the 2-axis tracker configuration has a higher energy gain, the 1-axis tracker has a more defined region of relevant energy processing in mid-currents.

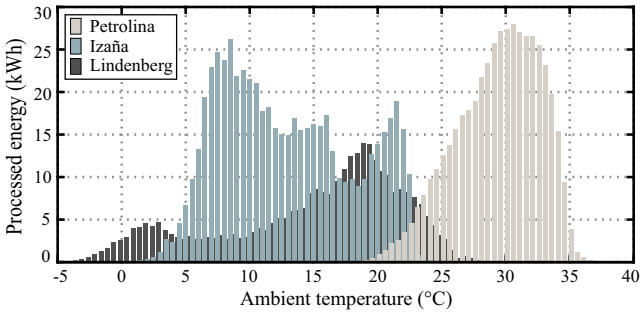

Fig. 12. One-year energy processed by a single PV module relative to ambient temperature.

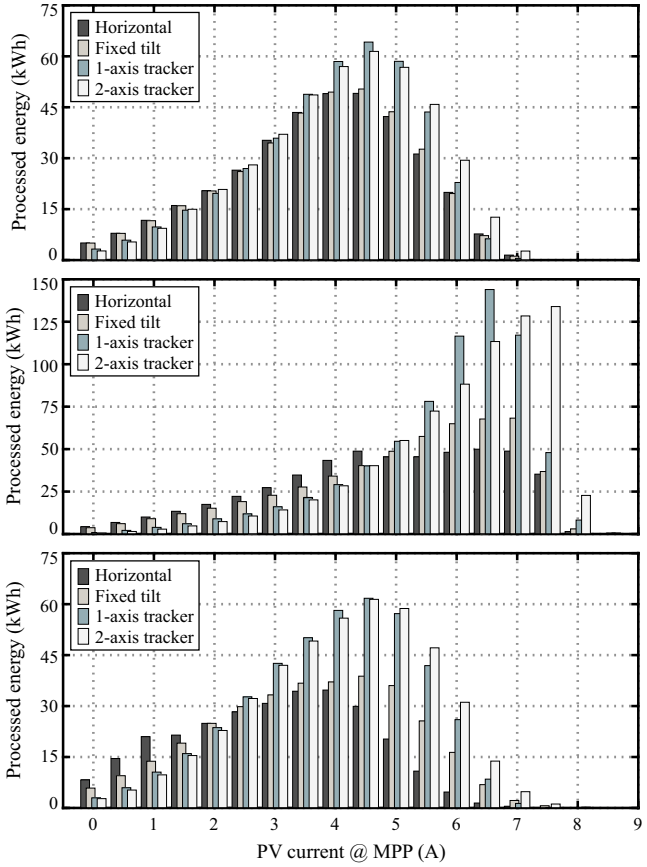

Fig. 13. One-year energy processed by a single PV module relative to the operating current at MPP, for (a) Petrolina, (b) Izaña, and (c) Lindenberg.

Due to its more constant weather condition, PV profile at Petrolina showed less variability among different PV mountings and smaller ranges of MPP current are responsible for most of the energy processing. Despite having very different irradiance and temperature profiles than Lindenberg, MPP current occurrences are somewhat similar.

The higher solar irradiance available at Izaña caused most energy processing in greater values and thinner ranges of MPP current. It is clear that mechanical trackers tend to decrease the range of currents significant to energy yield. Also, Fig. 13 shows that PV panel operation in its rated and maximum currents (Table 1) are extremely rare, and only a 2-axis tracker system at IZA resulted in substantial energy contribution in this range.

5.4. Weighted photovoltaic energy

Total generated energy of the experimental PV system, described in Section 2.3, was estimated as if it were operating under the mission profile conditions previously analyzed. The power processed by the SMC6000TL central inverter (SMA, 2016) was divided according to the load conditions of the California Energy Commission (CEC) for grid-tied inverters (Bower et al., 2004), where six power classes are considered (10%, 20%, 30%, 50%, 75%, and 100% of rated output power). Fig. 14 depicts the energy processed and active time of each power class in a one-year operation at PTR, IZA, and LIN for various mounting configuration.

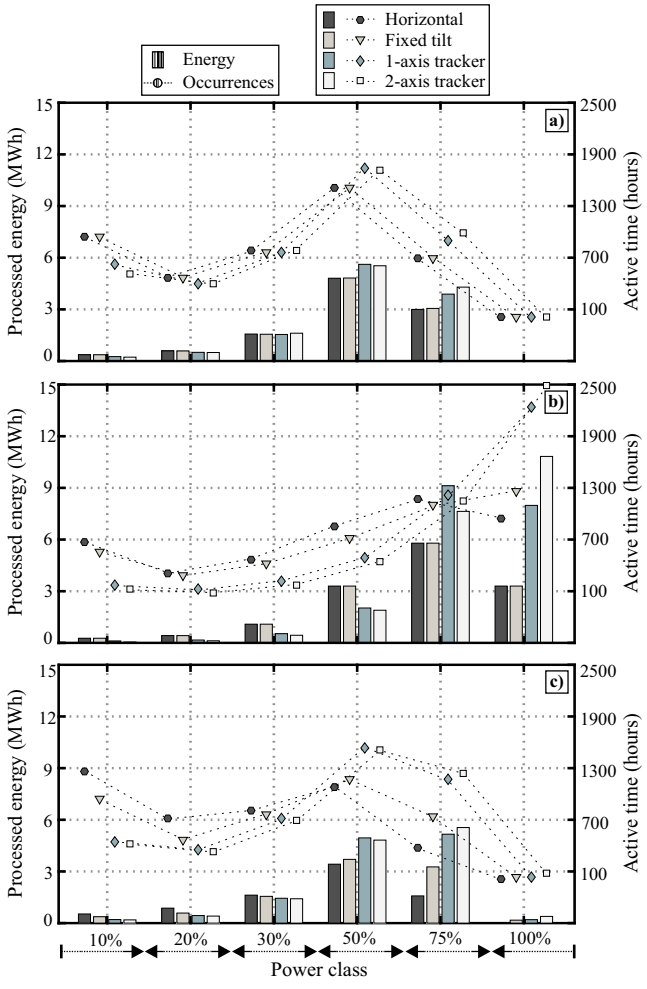

Fig. 14. PV energy processed and active time in one-year operation relative to CEC power classes for (a) Petrolina, (b) Izaña, and (c) Lindenberg.

Photovoltaic power converters are usually sized with respect to the system's nominal condition, which is the module maximum power in STC. However, PV panels hardly operate at maximum capacity due to thermal losses and irradiance variability, as can be seen in Figs. 11 and 13. Due to this over-dimensioning, Fig. 14 shows that the 100% power class had the least contribution in energy processing in almost all studied scenarios.

Moreover, traditional converter design techniques favor only rated power levels, which are not the most relevant in PV systems. Thus, in order to maximize annual energy processing, one must design the PV power converter so that its efficiency curve is similar to the distribution of its PV mission profile, as in Fig. 14. A design optimization can lead to higher efficiency in the power classes that contribute with most of the annual energy for a specific PV mission profile, which is analogous with matching array-to-inverter power ratio, as proposed by Rodrigo et al. (2016).

As can be seen in Fig. 14, power converters in PV plants with the use of mechanical trackers must be carefully designed, because the use of horizontal or fixed irradiance data may underestimate operation levels. Tracking alters not only critical and maximum values of energy and current but also the most relevant region for power processing. One should design a power converter that is more efficient and reliable in these regions according to the specific mission profile.

5.5. Final discussion

Designers should use a comprehensive approach to multiple areas of interest to model, design, and operate high-performance PV power plants. Power electronics elements play a fundamental role in this context since they are responsible for conditioning the solar energy in order to meet grid-quality standards and extract the maximum available power. Besides the technological challenges, power converters and inverters should be specified according to the local environment and specific PV system characteristics. Different design techniques can be used in order to enhance the overall performance of PV power converters. Nevertheless, one should first characterize an accurate mission profile to obtain a map of all the relevant conditions in which the power converter will operate.

Photovoltaic MP is composed of multiple analyses and results, and each one is relevant in different steps of the pre-design and design process. The definition of the PV system mounting type and orientation, as proposed in Section 4, serves to evaluate what the average annual power production profile will be. In addition, the use of long-term meteorological data aids to find the optimum tilt angles which will maximize solar energy yield. This information is valuable for sizing the photovoltaic power plant and performing financial feasibility analysis. Furthermore, the estimation of average and maximum values of PV current and voltage, as presented in Fig. 11 allows a proper choice and sizing of electronic and power elements in the DC/DC and/or DC/AC stages.

Moreover, previous knowledge of the most frequent $I \times V$ values and ambient temperatures, as shown in Figs. 11 and 12, enables the reliability-oriented design of power converters. With the mentioned analyses, the designer can perform lifetime estimations, select more appropriate topologies and/or component technologies, improve thermal performance and propose better heat-transfer solutions, and more. Lastly, estimation of the most relevant conditions in the power processing point-of-view, as presented in Figs. 11, 13, 14, empowers the designer to know in advance which region of operation of the power converter is the most valuable. The weighted processed power (Fig. 14) figure of merit provides needed information for executing optimized design of power converters.

6. Conclusions

The energy profile estimation of a PV power plant is a key requirement in pre-design phase and it provides essential information of the minimum, typical, and critical levels of PV operation, and, thus, the levels in which the power converter and its elements will operate.

This paper proposed a methodology for accurately characterizing the PV mission profile based on a long-period weather data and showed experimental modeling and validation of a PV system. Three locations with different climate conditions were analyzed, wherein energy processing was estimated for photovoltaic modules with fixed mounting, 1-axis, and 2-axis mechanical trackers.

A calculation of optimum tilt angles, for fixed and 1-axis tracker, based on the average annual incidence of solar irradiance was presented. A typical average year of ambient temperature and solar irradiance was built and various PV mission profiles were estimated based on mounting configuration and plant location. Experimental measurements from a 3.29 kW_P PV power plant were used for comparison, the validation of the methodology to estimate PV energy generation presented an error lower than 5%.

Climate and mounting-type influence on annual energy processing were analyzed. For sub-tropical locations, PV power processing occurred in a wider range of ambient temperature and the most frequent $I \times V$ operating points were not necessarily the ones responsible for most of the energy generation. In the tropical profile studied, a thinner range of PV current concentrates most of the power processing, especially with the use of mechanical trackers.

The methodology and analysis presented in this paper can be applied as a tool for obtaining useful information for the design of high performance and reliable PV power converters. Characterizing the mission profile of a photovoltaic power plant accurately allows the forecasting of critical and relevant operating conditions, hence, providing data that enables the improvement of power converter efficiency and reliability. Therefore, the proposed methodology for characterizing photovoltaic mission profile is an enabling tool for the design of modern PV power converters.

Acknowledgment

The authors thank the Baseline Solar Radiation Network for providing access to a quality database of significant measurements worldwide. This work received financial support from the Coordination of Superior Level Staff (CAPES).

References

Accetta, G., Piroddi, L., Ferrarini, L., 2012. Energy production estimation of a photovoltaic system with temperature-dependent coefficients. IEEE Int. Conf. Sustain Energy Technol. ICSET, 189–195. http://dx.doi.org/10.1109/ICSET.2012.6357396.

Beltrame, F., Dupont, FH., Sartori, HC., Cancian, EC., Rech, C., Pinheiro, JR., 2013. Efficiency optimization of DC/DC boost converter applied to the photovoltaic system. IECON Proc. (Indust. Electron Conf., 706–711 http://dx.doi.org/10.1109/IECON.2013.6699221.

Beltrame, F., Dupont, F.H., Sartori, H.C., Pinheiro, J.R., 2014. Design methodology to improve the converters' efficiency applied to photovoltaic systems. In: Proceedings, IECON 2014–40th Annu. Conf. IEEE Ind. Electron. Soc. 1397–1403. http://dx.doi.org/10.1109/IECON.2014.7048684.

Bower, W.N.L., Whitaker, C. Endecon E., Erdman, W.E.I., Behnke, M. (Bew E.I., Fitzgerald, M. (Institute for S.T., 2004. Performance test protocol for evaluating inverters used in grid-connected photovoltaic systems 41.

Chang, Y.P., Yang, L.D., 2012. Optimal tilt angle for PV modules considering the uncertainty of temperature and solar radiation. In: 2012 Int. Conf. Renew. Energy Res. Appl. ICRERA 2012. http://dx.doi.org/10.1109/ICRERA.2012.6477411.

Chen, C., Duan, S., Cai, T., Liu, B., 2011. Online 24-h solar power forecasting based on weather type classification using artificial neural network. Sol. Energy 85, 2856–2870. http://dx.doi.org/10.1016/j.solener.2011.08.027.

Grupo Clavijo, 2012. SP1000 Single-axis Solar Tracker - Technical Information Sheet.

Coelho, R.F., Concer, F., Martins, D.C., 2009. A proposed photovoltaic module and array mathematical modeling destined to simulation. IEEE Int. Symp. Ind. Electron. 1624–1629. http://dx.doi.org/10.1109/ISIE.2009.5214722.

Daut, I., Irwanto, M., Irwan, Y.M., Gomesh, N., Ahmad, N.S., 2011. Clear sky global solar irradiance on tilt angles of photovoltaic module in Perlis, Northern Malaysia. Int. Conf. Electr. Control Comput. Eng, 445–450. http://dx.doi.org/10.1109/INECCE.2011.5953923.

De Leon-Aldaco, S.E., Calleja, H., Aguayo Alquicira, J., 2015. Reliability and mission profiles of photovoltaic systems: a FIDES approach. IEEE Trans. Power Electron. 30, 2578–2586. http://dx.doi.org/10.1109/TPEL.2014.2356434.

Deb, J., Yohanis, Y.G., Norton, B., 2007. The impact of array inclination and orientation on the performance of a grid-connected photovoltaic system 32, 118–140. http://dx.doi.org/10.1016/j.renene.2006.05.006.

Demoulias, C., 2010. A new simple analytical method for calculating the optimum inverter size in grid-connected PV plants. Electr. Power Syst. Res. 80, 1197–1204. http://dx.doi.org/10.1016/j.epsr.2010.04.005.

Dupont, F.H., Rech, C., Pinheiro, J.R., 2012. A methodology to obtain the equations for the calculation of the weighted average efficiency applied to photovoltaic systems. In: 2012 10th IEEE/IAS Int. Conf. Ind. Appl. INDUSCON 2012. http://dx.doi.org/10.1109/INDUSCON.2012.6453445.

Faranda, R.S., Hafezi, H., Leva, S., Mussetta, M., Ogliari, E., 2015. The Optimum PV Plant for a Given Solar DC/AC Converter 4853–4870. http://dx.doi.org/10.3390/en8064853.

Freitas, S., Serra, F., Brito, M.C., 2015. Pv layout optimization: string tiling using a multi-objective genetic algorithm. Sol. Energy 118, 562–574. http://dx.doi.org/10.1016/j.solener.2015.06.018.

Pairan GmbH, 2015. Tracking system CPV40 - Technical Information.

Grupo Clavijo, 2012. SR10 Dual-axis solar tracker - Technical Information.

Gulin, M., Pavlovic, T., Vašak, M., 2017. A one-day-ahead photovoltaic array power production prediction with combined static and dynamic on-line correction. Sol. Energy 142, 49–60.

Huld, T., Müller, R., Gambardella, A., 2012. A new solar radiation database for estimating PV performance in Europe and Africa. Sol. Energy 86, 1803–1815. http://dx.doi.org/10.1016/j.solener.2012.03.006.

IRENA, 2012. Renewable Energy Technologies: Cost Analysis Series – Solar Photovoltaics. International Renewable Energy Agency.

Khan, M.M., Ahmad, M.J., 2012. Estimation of global solar radiation using clear sky radiation in Yemen. J. Eng. Sci. Technol. Rev. 5, 12–19.

Klein, G., Baumgartner, F.P., Häberlin, H., Bründlinger, R., Bletterie, B., Goeldi, B., Schmidt, H., Burger, B., 2009. Are we Benchmarking Inverters on the Basis of Outdated Definitions of the European and CEC Efficiency? 24th Eur. Photovolt. Sol. Energy Conf. 21-25 Sept. 2009, Hamburg, Ger. 3638–3643. http://dx.doi.org/10.4229/24thEUPVSEC2009-4BV.1.10.

Kolar, J.W., Biela, J., Miniböck, J., 2009. Exploring the Pareto Front of Multi-Objective Single-Phase PFC Rectifier Design Optimization - 99.2% Efficiency vs. 7kW/dm3 Power Density. In: International Power Electronics and Motion Control Conference. pp. 1–21.

Lewis, G., 1987. Optimum tilt of solar collectors, Solar and Wind Technology.

Long, C.N., Dutton, E.G., 2004. BSRN Global Network recommended QC tests, V2.0 [WWW Document]. http://bsrn.awi.de/data/quality-checks.html (accessed 5.23.16).

Meca Solar, 2014a. High Tech Solar Trackers 1-Horizontal Axis - Technical Datasheet.

Meca Solar, 2014b. High Tech Solar Trackers 1-axis polar Technical Datasheet.

Mondol, J.D., Yohanis, Y.G., Norton, B., 2006. Optimal sizing of array and inverter for grid-connected photovoltaic systems. Sol. Energy 80, 1517–1539. http://dx.doi.org/10.1016/j.solener.2006.01.006.

Moore, L.M., Post, H.N., 2008. Five Years of Operating Experience at a Large, Utility-scale Photovoltaic Generating Plant z 249-259. doi: 10.1002/pip.

Paulescu, M., Paulescu, E., Gravila, P., Badescu, V., 2013. Weather modeling and forecasting of PV systems operation. Green Energy Technol. 103. http://dx.doi.org/10.1007/978-1-4471-4649-0.

Peippo, K., Lund, P.D., 1994. Optimal sizing of grid-connected PV-systems for different climates and array orientations: a simulation study. Sol. Energy Mater. Sol. Cells 35, 445–451. http://dx.doi.org/10.1016/0927-0248(94)90172-4.

Pesos.Solar.Products, 2015. SunFlex SD tracking systems Technical information for control systems SF20-60SD.

Rahman, S.A., Vanderheide, T., Varma, R.K., 2014. Generalised model of a photovoltaic panel. IET Renew. Power Gener. 8, 217–229. http://dx.doi.org/10.1049/iet-rpg.2013.0094.

Reda, I., Andreas, A., 2008. Solar Position Algorithm for Solar Radiation Applications (Revised). Nrel/Tp-560-34302, 1–56. http://dx.doi.org/10.1016/j.solener.2003.12.003.

Reindl, D.T., Beckman, W.A., Duffie, J.A., 1990. Evaluation of hourly tilted surface radiation models. Sol. Energy 45, 9–17. http://dx.doi.org/10.1016/0038-092X(90)90061-G.

Rhodes, J.D., Upshaw, C.R., Cole, W.J., Holcomb, C.L., Webber, M.E., 2014. ScienceDirect A multi-objective assessment of the effect of solar PV array orientation and tilt on energy production and system economics. Sol. Energy 108, 28–40. http://dx.doi.org/10.1016/j.solener.2014.06.032.

Ristow, A., Begović, M., Pregelj, A., Rohatgi, A., 2008. Development of a methodology for improving photovoltaic inverter reliability. IEEE Trans. Ind. Electron. 55, 2581–2592. http://dx.doi.org/10.1109/TIE.2008.924017.

Rodrigo, P.M., Velázquez, R., Fernández, E.F., 2016. DC / AC conversion efficiency of grid-connected photovoltaic inverters in central Mexico. Sol. Energy 139, 650–665. http://dx.doi.org/10.1016/j.solener.2016.10.042.

Sartori, H.C., Beltrame, F., Figueira, H.H., Baggio, J.E., Pinheiro, J.R., 2013. Power density comparative analysis concerning to three transistor technologies applied to a CCM PFC BOOST converter using optimization techniques. In: 2013 Brazilian Power Electronics Conference. IEEE, pp. 1317–1323. http://dx.doi.org/10.1109/COBEP.2013.6785286.

Scarpa, V.V.R., Araújo, S. V, Sahan, B., Zacharias, P., 2011. Achieving Higher Power Density in DC-DC Converters for Photovoltaic Applications. In: Proc. 2011–14th Eur. Conf. Power Electron. Appl. (EPE 2011).

Schmithüsen, H., Sieger, R., König-Langlo, G., 2012. BSRN Toolbox V2.0 - a tool to create quality checked output files from BSRN datasets and station-to-archive files. http://dx.doi.org/10.1594/PANGAEA.774827.

Sintamarean, N.C., Blaabjerg, F., Wang, H., Yang, Y., 2014. Real field mission profile oriented design of a SiC-Based PV-inverter application. IEEE Trans. Ind. Appl. 50, 4082–4089. http://dx.doi.org/10.1109/TIA.2014.2312545.

Siraki, A.G., Pillay, P., 2012. Study of optimum tilt angles for solar panels in different latitudes for urban applications. Sol. Energy 86, 1920–1928. http://dx.doi.org/10.1016/j.solener.2012.02.030.

Skoplaki, E., Palyvos, J.A., 2009a. Operating temperature of photovoltaic modules: a survey of pertinent correlations. Renew. Energy 34, 23–29. http://dx.doi.org/10.1016/j.renene.2008.04.009.

Skoplaki, E., Palyvos, Ja., 2009b. On the temperature dependence of photovoltaic module electrical performance: a review of efficiency/power correlations. Sol. Energy 83, 614–624. http://dx.doi.org/10.1016/j.solener.2008.10.008.

SMA, 2016. Sunny Mini Central 6000TL/7000TL/8000TL Technical Data.

SPE, Solar Power Europe, 2016. Global Market Outlook for Solar Power 2016–2020. http://www.solarpowereurope.org (accessed 7.12.16) Brussels.

Vergura, S., 2015. Scalable model of PV cell in variable environment condition based on the manufacturer datasheet for circuit simulation. In: 2015 IEEE 15th Int. Conf. Environ. Electr. Eng. EEEIC 2015 - Conf. Proc., pp. 1481–1485. http://dx.doi.org/10.1109/EEEIC.2015.7165390.

Villalva, M.G.G., Gazoli, J.R.R., Filho, E.R.R., 2009. Comprehensive approach to modeling and simulation of photovoltaic arrays. IEEE Trans. Power Electron. 24, 1198–1208. http://dx.doi.org/10.1109/TPEL.2009.2013862.

Wang, H., Zhou, D., Blaabjerg, F., 2013. A reliability-oriented design method for power electronic converters. Appl. Power Electron. Conf. Expo., 2921–2928 http://dx.doi.org/10.1109/APEC.2013.6520713.

WRMC-BSRN, 2017. BSRN Data Retrieval [WWW Document]. http://bsrn.awi.de/data/data-retrieval-via-pangaea/ (accessed 1.1.17).

Yadav, A.K., Malik, H., 2015. Optimization of Tilt Angle for installation of Solar Photovoltaic system for six sites in India. In: International Conference on Energy Economics and Environment.

Zhang, P., Wang, Y., Xiao, W., Li, W., 2012. Reliability evaluation of grid-connected photovoltaic power systems. IEEE Trans. Sustain. Energy 3, 379–389. http://dx.doi.org/10.1109/TSTE.2012.2186644.

ZVEI, 2008. Handbook for Robustness Validation of Automotive Electrical / Electronic Modules, Zentralverband Elektrotechnik- und Elektronikindustrie e. V. Electronic Components and Systems Division, Frankfurt.